Attosecond timescale analysis of the dynamics of two-photon double ionization of helium

E. Foumouo, P. Antoine, H. Bachau, B. Piraux

New Journal of Physics

Attosecond timescale analysis of the dynamics of two-photon double ionization of helium

Emmanuel Foumouo[1,3]**, Philippe Antoine**[1]**,
Henri Bachau**[2] **and Bernard Piraux**[1]

[1] Laboratoire de Physique Atomique, Moléculaire et Optique, unité PAMO,
Université catholique de Louvain, 2 chemin du cyclotron,
B-1348 Louvain-la-Neuve, Belgium
[2] Centre Lasers Intenses et Applications, Université Bordeaux I-CNRS-CEA,
33405 Talence Cedex, France
E-mail: efoumouo@yahoo.fr and foumouo@pamo.ucl.ac.be

Abstract. We consider the two-photon double ionization (DI) of helium and analyze electron dynamics on the attosecond timescale. We first re-examine the interaction of helium with an ultrashort XUV pulse and study how the electronic correlations affect the electron angular and energy distributions in the direct, sequential and transient regimes of frequency and time duration. We then consider pump–probe processes with the aim of extracting indirect information on the pump pulse. In addition, our calculations show clear evidence for the existence under certain conditions of direct two-color DI processes.

[3] Author to whom any correspondence should be addressed.

Contents

1. Introduction

The generation of high-order harmonics of a strong infrared laser field appears to be the most efficient process to generate single attosecond (as) XUV pulses [1]. With the use of carrier-envelope phase stabilization and few-cycle laser systems, it is now possible to produce XUV pulses whose duration is shorter than 250 as [2]. The production of such pulses provides new routes to time-domain studies of multi-electron dynamics in atoms and molecules. The feasibility of such studies has been demonstrated by the pioneer experiment of Drescher *et al* [3] who studied in real time the relaxation of krypton M-shell vacancies. In this experiment, it is actually the coupling of a bound state to various continua that is explored in the time-domain with attosecond resolution. The characteristic timescales which are given by the corresponding transition linewidths, are usually of the order of a femtosecond.

In the present contribution, we consider the interaction of He with ultrashort XUV pulses and focus on the two-photon double ionization (TPDI) process. This process has recently become the subject of intense theoretical interest (see [4] and other references therein) as well as the target of new experiments with high-order harmonic generation [5] and free-electron laser source (FLASH) in Hamburg [6, 7]. TPDI total cross-sections have been measured [5, 6] for the case of direct TPDI of He. The measure of the momentum distribution of the recoil ion in a cold target recoil ion momentum spectroscopy (COLTRIMS) experiment provides information on the energy sharing and the direction of emission of the two ejected electrons in Ne TPDI [7]. Here, it is the electron correlation in the ground state of He which is explored in the time domain. In order to define a characteristic time scale associated with the electron correlation in a given bound state, we introduce what we call the dielectronic interaction energy E_{int}, defined as the difference between the 'exact' energy of this state of He and the corresponding energy of a 'model helium' in which both electrons are independent. For the He ground state E_{int} is about 1.1 au. Note that we use the term 'dielectronic interaction energy' rather than 'correlation energy' employed in previous papers to avoid possible confusion. Indeed, the correlation energy often refers to the difference between the exact and the Hartree–Fock energy. For the He ground state, this correlation energy is much less than E_{int}. E_{int} actually represents the total amount of energy that both electrons can exchange during the ionization process. The characteristic timescale τ associated with the electron correlation in a given bound state is then defined as $2\pi/E_{int}$. For He in its ground state, this characteristic timescale is of the order of 140 as.

For long pulses, the TPDI process may be direct or sequential. For photon energies larger than 2 au, it is possible for the two electrons to escape sequentially, i.e. each electron absorbs a single photon and escapes one after the other. In this sequential regime, there is no need for electron correlation and it is the first ejected electron that carries the dielectronic interaction energy E_{int} [8]. In other words, the residual ion has time to relax into the ground state of He$^+$ before the second ionization. For photon energies below 2 au and above the TPDI threshold (1.45 au), the sequential process is energetically forbidden and both electrons must share the dielectronic interaction energy to escape. Probing the electron correlation amounts therefore to analyzing how this dielectronic interaction energy is partitioned between the electrons. Direct and sequential processes may be distinguished by the fact that the probability of direct TPDI is proportional to the time duration of the pulse, whereas in the sequential regime, the probability of TPDI is proportional to the square of the pulse duration. In a previous publication [9], we have shown that there is a third regime called transient which is neither direct nor sequential. In this mode the dependence of the probability of TPDI on the pulse duration is not linear or quadratic. This regime manifests itself when the pulse duration becomes extremely short, i.e. of the order of the characteristic timescale τ. In particular, we have studied, for photon energies above 2 au, how the electron energy distributions and the ion yield for TPDI of He in its ground state change for ultrashort pulse duration. Note that in the sequential regime, the process of TPDI may be viewed as a pump–probe process within a single pulse: the first photon ionizes He while the second one 'probes' the initial photoionization process. In the present contribution, we study the TPDI of He ^{1}S by two (not necessarily ultrashort) XUV pulses. We analyze both the electron energy distribution and the ion yield as a function of the time delay between the pulses. In particular, we show that some time delays lead to dynamical effects similar to what is expected when He interacts with a single attosecond pulse.

The present contribution is organized as follows. In the first section, we give a short account of our theoretical approach. In the next two sections, we briefly review the main features of the direct and sequential TPDI process and then consider the third regime in more detail. In particular, we elucidate the actual role of the electron correlations by analyzing the electron energy and angular distributions. In the fourth section, we consider the interaction of He with two XUV pulses and discuss the atomic response in detail. We conclude in section 5. Unless stated, atomic units are used throughout this paper.

2. Theoretical approach

Our theoretical approach is based on the solution of the time-dependent Schrödinger equation (TDSE):

$$i\frac{\partial}{\partial t}\Psi(\vec{r}_1, \vec{r}_2, t) = \left[-\frac{1}{2}\nabla_{r_1}^2 - \frac{1}{2}\nabla_{r_2}^2 - \frac{2}{r_1} - \frac{2}{r_2} + \frac{1}{r_{12}} + D_G(t)\right]\Psi(\vec{r}_1, \vec{r}_2, t), \tag{1}$$

where r_1 and r_2 are the radial coordinates of both electrons and $r_{12} = |\vec{r}_1 - \vec{r}_2|$ is the interelectronic distance. $D_G(t)$ describes the dipole interaction of the system with the oscillating field either in the length gauge ($G \equiv L$) or in the velocity gauge ($G \equiv V$):

$$D_L(t) = \vec{E}(t) \cdot (\vec{r}_1 + \vec{r}_2), \tag{2}$$

$$D_V(t) = -i\vec{A}(t) \cdot (\vec{\nabla}_1 + \vec{\nabla}_2). \tag{3}$$

$\vec{A}(t)$ denotes the vector potential and $\vec{E}(t) = \hat{z} E_0 f(t) \sin(\omega t + \phi)$ the electric field which oscillates at the frequency ω with a phase ϕ and which is assumed to be linearly polarized along the z-axis. $f(t)$ is the pulse envelope given by:

$$f(t) = \cos^2(t/\tau), \quad |t| \leqslant \pi \frac{\tau}{2},$$
$$= 0, \quad |t| > \pi \frac{\tau}{2}. \tag{4}$$

In this expression, $\pi\tau$ represents the total duration of the pulse expressed as an integer number of optical periods, we have:

$$\vec{A}\left(\pi \frac{\tau}{2}\right) = -\int_{-\pi(\tau/2)}^{\pi(\tau/2)} dt \, \vec{E}(t) = 0, \tag{5}$$

for any pulse duration and phase. This means that even for few-cycle pulses, there is no static field component. This prevents possible problems related to the gauge invariance [10]. In addition, it is easy to show that the spectral width of such a pulse, defined as the FWHM of the square of the Fourier transform of $\vec{E}(t)$, is given by $1.44\omega/n$ where the integer n is the total number of optical cycles within the pulse.

Our method to solve the TDSE (equation (1)) has been described in great detail in [11]. Here, we only present a short summary. We first expand the full wavepacket of the system $\Psi(\vec{r}_1, \vec{r}_2, t)$ in terms of its field-free eigenstates. The wavefunctions associated with these eigenstates are calculated within a spectral method that consists in diagonalizing the atomic Hamiltonian in a basis of products of one-electron square integrable functions of the radial coordinates r_1 and r_2 and bipolar harmonics of the electron angular coordinates. The square integrable functions are either Coulomb Sturmian functions or B-splines. The Coulomb Sturmian functions $S_{n,\ell}^k(r)$ for a given angular momentum ℓ and radial index n are defined by:

$$S_{n,\ell}^{\kappa}(r) = N_{n,\ell}^{\kappa} \, r^{\ell+1} e^{-\kappa r} L_{n-\ell-1}^{2\ell+1}(2\kappa r), \tag{6}$$

where $N_{n,\ell}^{\kappa}$ is a normalization constant and $L_{n-\ell-1}^{2\ell+1}(2\kappa r)$ a Laguerre polynomial. The wavevector κ plays the role of a scaling factor [12] while the index n varies between $\ell+1$ and $N+\ell$ where N is the number of Coulomb Sturmian functions per electron for a given ℓ. It is important to stress that these functions, which form a complete and discrete basis, are solutions of the Sturm–Liouville eigenvalue problem associated with the radial stationary Schrödinger equation for an hydrogenoid system. The B-splines functions [13] $B_n^k(r)$ of order k are piecewise polynomials of degree $k-1$. The index n varies from 1 to N_b where N_b is the number of B-splines per electron. The N_b B-spline functions are spanned, along the radial axis, in a box defined from $r = 0$ to R_{max}. The B-spline sequence is chosen in such a way that $B_1^k(0) = B_{N_b}^k(R_{max})$ in order to satisfy the correct boundary conditions within the box. The full wavepacket which initially coincides with the initial state of He is then propagated in time by means of an explicit fifth order embedded formula of Runge–Kutta type.

Once the initial wavepacket has been propagated in time until the end of the interaction with the pulse, we have to calculate both the single and the double ionization (DI) probabilities. This problem remains a real challenge for all theoretical approaches. On the one hand, the single and double continua of He may be degenerate in energy and, on the other hand, the positive energy eigenstates of the Hamiltonian of He contain necessarily both single and double continuum components since our basis has a finite size and does not describe the electron pair

in the asymptotic region. In addition, these asymptotic conditions for complete break up are not known. In order to calculate the total probability for DI, we subtract the total probability for single escape from the all-inclusive probability for breakup which in turn is obtained from the final wavepacket without reference to the boundary conditions. To calculate the total and partial probabilities for single escape, we use the Jacobi-matrix method [14] to generate in the Coulomb Sturmian basis a multichannel scattering wavefunction that describes accurately the single continuum of He while incorporating the correct asymptotic conditions. Projecting the final wavepacket $\Psi(t)$ at the end of the pulse on this function provides a tool to disentangle the single-ionization and DI components denoted by $\Psi_{si}(t)$ and $\Psi_{di}(t)$ respectively. In order to calculate the electron energy and angular distribution for double-escape, we project the DI component $\Psi_{di}(t)$ on the wavefunction Φ which describes two 'non-interacting electrons' moving in the field of an unscreened He nucleus. Φ is in fact a product of two one-electron Coulomb wavefunctions with effective charge 2. Because Φ is only an approximate final-state wavefunction for two asymptotically free electrons and is not orthogonal to the 'exact' single-ionization and bound-state-channel wavefunctions, it is essential to isolate the double-escape wavepacket $\Psi_{di}(t)$ before projecting on to Φ. However, as soon as the two-photon single-ionization component becomes small compared to the DI, i.e. for higher frequencies in the sequential regime, this procedure of subtraction is no longer essential and the projection of the final wavepacket on the function Φ is sufficient. We have checked that our estimates for the single- and double-electron escape probabilities are converged with respect to the basis size and are gauge independent.

In order to probe how electron correlations in the ground state of He affect the double-escape process, we have developed a simple model in which electron correlations enter only in the ground state of He. This model is based on the lowest order time-dependent perturbation theory. This is justified since in the high frequency and low intensity regime considered here, the ponderomotive shift of the electrons is negligible compared to the photon energy. For TPDI, the probability amplitude reads:

$$U^{(2)} = -\sum_\alpha \langle \Psi_f | z_1 + z_2 | \Psi_\alpha \rangle \langle \Psi_\alpha | z_1 + z_2 | \Psi_i \rangle G(E_0, \omega, \phi, E_i, E_\alpha, E_f), \qquad (7)$$

where the function G is given by:

$$G(E_0, \omega, \phi, E_i, E_\alpha, E_f) = \int_{-T/2}^{T/2} d\tau_1 E_0 f(\tau_1) \sin(\omega\tau_1 + \phi) e^{i\omega_{f\alpha}\tau_1}$$

$$\times \int_{-T/2}^{\tau_1} d\tau_2 E_0 f(\tau_2) \sin(\omega\tau_2 + \phi) e^{i\omega_{\alpha i}\tau_2}. \qquad (8)$$

In this expression, T represents the optical period and $\omega_{f\alpha} = E_f - E_\alpha$ and $\omega_{\alpha i} = E_\alpha - E_i$ with E_i, E_α and E_f the initial, the intermediate and the final state energy, respectively. The wavefunction of the initial state Ψ_i is written as follows:

$$\Psi_i(\vec{r_1}, \vec{r_2}) = \sum_{l,\nu,n} \phi_{\nu,n}^{l,l} \mathcal{A} F_{\nu,n}^{l,l}(r_1, r_2) \Lambda_{l,l}^{0,0}(\Omega_1, \Omega_2), \qquad (9)$$

where the coefficients $\phi_{\nu,n}^{l,l}$ are calculated by diagonalizing the atomic Hamiltonian of He. $\mathcal{A}$ is the antisymmetrization operator and $\Lambda_{l,l}^{0,0}(\Omega_1, \Omega_2)$ the bipolar harmonics of the angular coordinates of both electrons. The radial function $F_{\nu,n}^{l,l}(r_1, r_2)$ is written as a product of two hydrogenic bound states of principal quantum number ν and n respectively:

$$F_{\nu,n}^{l,l}(r_1, r_2) = \psi_{\nu,l}(r_1)\psi_{n,l}(r_2). \qquad (10)$$

Let us stress that the above expression (9) for Ψ_i is not correct because this expansion does not contain continuum states. However, it contains some radial and angular correlation. In this calculation of $\Psi_i(\vec{r}_1, \vec{r}_2)$, we have included 4 pairs (ℓ, ℓ) of the electron angular momenta $((0, 0),$ $(1, 1), (2, 2)$ and $(3, 3))$ and taken both ν and n varying from $1 + \ell$ to $4 + \ell$. Upon these conditions, the ground state energy is -2.84 au. The intermediate states Ψ_α and the final state Ψ_f can be defined in good approximation as an antisymmetrized product of bound or/and Coulomb states because the TPDI process is dominated by transition channels that require no interaction between the electrons in the sequential regime [8]. We have tested this model by comparing the results with those obtained by the approach described at the beginning of this section. The agreement is good both qualitatively and quantitatively. In addition, this model also gives reasonable results in the direct regime.

3. Electron correlations in TPDI

3.1. Direct regime

By using our spectral method together with Jacobi-matrix calculations, we have shown recently [15] that in the range of photon energies from 39.5 to 54.4 eV, the dominant TPDI process is a back-to-back electron ejection along the field polarization axis at equal energies. This results from the absorption of two photons by the electron pair in the presence of a dynamically screened nucleus. Very close to the 39.5 eV threshold, each electron must maximally screen the other in order to overcome the Coulomb attraction from the nucleus. As the photon energy rises from 39.5 to 54.4 eV, dynamical screening becomes less critical and each electron can escape partially independently of the other. As a result, the phase space available to the electrons increases and consequently, the rate for double escape rises. The role of the dynamical screening manifests itself in the electron energy distributions. Close to the 39.5 eV threshold and up to a photon energy of about 48 eV, the distribution exhibits a maximum at the equal energy sharing while above 48 eV, this distribution becomes more U-shaped. This dynamical screening [16] is a direct consequence of the radial correlations whereas the strongly favored back-to-back emission is a consequence of the angular correlations. In addition, the symmetry of the initial or final state also plays an important role regarding the pertinence of the above mechanism. Indeed, such a mechanism is not dominant in the one-photon DI of He because the final state has a node when both electrons are emitted back-to-back at exactly the same energy.

3.2. Sequential and transient regimes

For photon energies larger than 54.4 eV (2 au), TPDI of He is either direct or sequential. In the case of the direct process, the electrons share the excess energy E_{ex} leading to a relatively uniform electron energy distribution while the sequential process leads to an energy distribution that exhibits two peaks of energies E_1 and E_2, resulting from the ionization of He$^+$ and He, respectively. Figure 1 shows the schematic diagram of these processes; in figure 1(a), the direct path is represented by dashed arrows, it leads to excitation-ionization and DI channels where the electrons share the excess energy E_{ex}. The sequential path, also represented in figure 1(a), produces electrons with energies E_1 and E_2 ($E_1 + E_2 = E_{ex}$). The direct and sequential processes are entangled, we will discuss their relative importance. The associated electron spectrum is represented in figure 1(b). The peaks E_1 and E_2 are separated in energy by E_{int}, i.e. the total
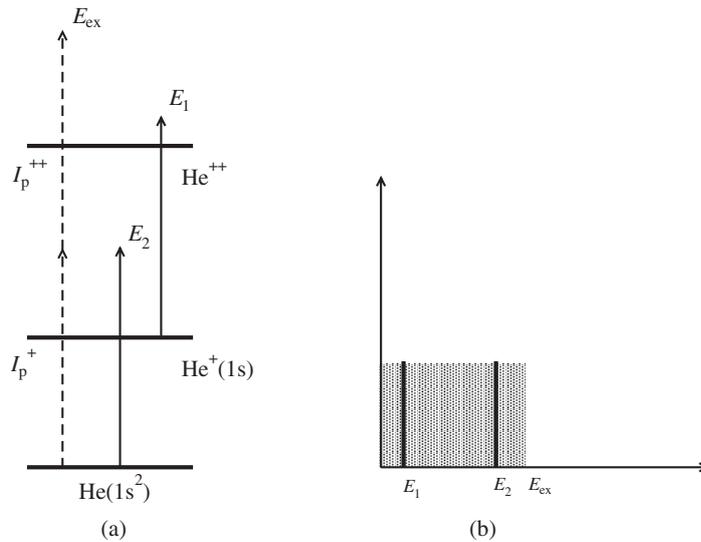
Figure 1. A schematic diagram of the TPDI process. Figure 1(a) represents the direct and sequential pathways. Figure 1(b) represents the region corresponding to direct ionization, ranging from the energy 0 up to the excess energy E_{ex}. The figure also shows two peaks corresponding to sequential ionization, located at the positions E_1 and E_2 (with $E_{ex} = E_1 + E_2$). The normalization of direct and sequential yields is arbitrary.

dielectronic interaction energy in He($1s^2$) (about 1.1 au). It has been pointed out that, by contrast to one-photon DI, TPDI occurs without correlations. Nevertheless let us stress that, in the model of non-interacting electrons, the electron spectrum shows a single peak ($E_1 = E_2$) for $\omega > 2$ au, while the direct process is energetically forbidden for $\omega < 2$ au. Therefore it is *a priori* obvious that the dielectronic interaction plays a crucial role in TPDI, but it is different from its role in the one-photon DI case [17].

Before considering the transient regime of the ultrashort pulse durations, we recall a previous study where the role of the electron correlations has been discussed within the lowest order perturbation theory [8]. In this approach, the He ground state is represented by $1s^2$, i.e. a product of two hydrogenic orbitals 1s. The other states are the single continuum state He($1skp$) and double continuum He($kpk'p$), also represented by hydrogenic orbitals (all orbitals are calculated with $Z = 2$). In this approximation the energy $E_{1s^2}^0$ of the ground state would then be given by $2E_{1s}^0 + \langle 1s^2|1/r_{12}|1s^2 \rangle$ where E_{1s}^0 is the hydrogenic energy of 1s and $\langle 1s^2|1/r_{12}|1s^2 \rangle$ the electron interaction energy. This model includes the resonant transitions underlying the sequential process; one-photon ionization of He($1s^2$) followed by the ionization of He$^+$(1s). Here it is important to emphasize that the zeroth order perturbation theory in $1/r_{12}$ approximation is different from the fully electron independent model where the ground state energy is $2E_{1s}^0$. Within zeroth order perturbation theory, the unique role of the electron interaction energy is to shift the ground state upward. Using the formalism of the resolvent operator $G(z)$ and a square pulse of length T, we apply the standard method where the evolution operator $U_{FI}(T)$ is obtained as the inverse Laplace transform of $G_{FI}(z)$. Details are given in [8] where the lower level is the He ($2s^2$) autoionizing state with lifetime $1/\Gamma$ while the upper one is the He$^+$(2s) threshold. Setting $\Gamma = 0$ and replacing the 2s orbital by 1s a parallel treatment
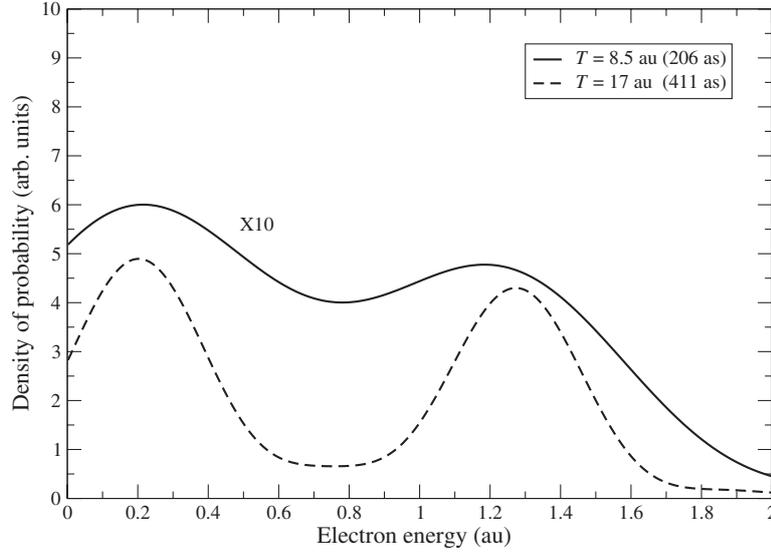
Figure 2. Electron energy spectrum calculated within the zeroth order perturbation theory in $1/r_{12}$ for a photon energy of 2.2 au and for two pulse durations (see the insert).

applies here. We have shown in [8] that, for $T = \infty$, it is possible to derive an analytical expression for the photoelectron energy spectrum, it reads:

$$|U_{k,k'}(T \to \infty)|^2 \propto \frac{|\langle k\mathrm{p}|\mu|1\mathrm{s}\rangle\langle k'\mathrm{p}|\mu|1\mathrm{s}\rangle|^2}{[(E_k + E_{k'} - E_{\mathrm{ex}})^2 + (1/4)\gamma_{\mathrm{He}}^2][(E_k - E_1)^2 + (1/4)\gamma_{\mathrm{He}^+}^2]}, \tag{11}$$

where γ_{He} and γ_{He^+} are the photoionization widths of He and He^+, respectively. $\langle k\mathrm{p}|\mu|1\mathrm{s}\rangle$ represents the dipole coupling between the 1s orbital and the $k\mathrm{p}$ continuum. E_k and $E_{k'}$ are the energies of the ejected electrons. We recognize in equation (11) the channel where each electron absorbs one photon. It is clear that the dipoles are different from zero, whether we use hydrogenic orbitals or not. The electron spectrum associated with equation (11) shows two peaks whose effective widths are the result of a convolution (see figure 2 in [8]). We have also evaluated $U_{\mathrm{FI}}(T)$ for finite values of T; figure 2 shows the electron spectrum associated with TPDI for $T = 8.5$ au and $T = 17$ au and for a photon energy of 2.2 au. The ionization threshold has been arbitrarily placed at 0.903 au above the He fundamental state. The spectrum is dominated by two peaks placed at the expected positions $E_1 = 0.2$ au and $E_2 = 1.3$ au; by contrast with equation (11) their width is given by the laser bandwidth, which is much larger than the photoionization widths. At $T = 8.5$ au, we note that the peaks slightly move towards each other. Regarding the TPDI rate, we have checked that it varies like T^2, in agreement with sequential DI. While the sequential TPDI is expected to dominate for long pulse durations, it is interesting to compare the present model with a more sophisticated calculation for short pulses in the transient regime; this is investigated below with our spectral method using B-spline functions.

In previous work [18, 19] we have shown that, for $\hbar\omega > 2$ au and pulse durations T of the order of $2\pi/E_{\mathrm{int}}$ or less, TPDI occurs while both electrons strongly interact and the concept of sequential ionization loses its pertinence. In the latter case, the DI rate [9] and the electron

energy spectrum [20, 21] differ significantly from the long pulse regime. Note that in the transient regime, i.e. for very short pulses, the field bandwidth is of the order of the field frequency so that the notion of photon loses its meaning. In fact, for pulse durations of the order of or less than $2\pi/E_{int}$, hereafter called the dielectronic interaction time, we enter the transient regime. Note that this dielectronic interaction time, which is of the order of 140 as for the helium ground state, can be longer for other elements, such as for instance beryllium where it is about 500 as [21].

We report here on TPDI electron energy and angular distributions calculated by using our spectral method based on the B-spline functions. The results have been obtained by projecting the final wavepacket at the end of the pulse on a product of Coulomb functions with effective charge 2. As indicated before, this procedure is justified for average field frequencies larger than 2 au. The calculations have been performed at various intensities. Channels populated through the absorption of three photons have been included in TDSE calculations. We have checked that they play a negligible role. It is worth noting that, in the case of neon, sequential three-photon DI has been shown to compete with direct TPDI at rather low intensities [6, 7]. This might be due to the presence of a resonant transition in Ne$^+$. The present context is different but we have carefully checked that, for both direct and sequential two-electron ejection regimes, two-photon absorption dominates up to the maximum intensity used in this work (i.e. 10^{14} W cm^{-2}). In all cases, we have also checked that ionization is well below the saturation regime. Within this context the final doubly ionized channels have symmetries $^1S^e$ and $^1D^e$ and the intermediate one (populated from the He (1s^2) state) has the symmetry $^1P^o$. For the $^1S^e$ states, we have included the following electron angular momentum pairs (ℓ_1, ℓ_2): (0, 0), (1, 1), (2, 2) and (3, 3); the energy of the ground state is -2.903 au. For the $^1P^o$ states, we have taken into account the pairs (0, 1), (1, 2) and (2, 3) and for the $^1D^e$ states, the pairs (0, 2), (1, 1), (1, 3), (2, 2) and (3, 3). For the He ground state, (0, 0) is the dominant electron angular momentum pair. Therefore, the one-photon transition to (0, 1) plays a major role and the (0, 0), (1, 1) and (0, 2) pairs dominate in the final double continuum, as we will see below. The $^1F^o$ channel, populated through three-photon absorption, is also included in the calculations but, as explained above, it plays a minor role. Note that the main constraint regarding our B-spline basis is the size of the box, that has to be large enough to avoid the bouncing back of the wavefunction on the boundaries, here at $R_{max} = 30$ au. Figure 3 shows the total and partial densities of probability and the dominant angular contributions, in the insert L, l_1 and l_2 refer to respectively the total angular momentum and to angular components of the final double continuum state, represented by a product of two Coulomb functions. The DI density of probability reads [20]:

$$\frac{d^2 P_{l_1,l_2}^{L,M}}{dE_k dE_{k'}} = |\langle \mathcal{A}(\psi_{E_k}^{l_1}(r_1) \psi_{E_{k'}}^{l_2}(r_2) \mathcal{Y}_{l_1,l_2}^{L,M}(1,2)) | \Psi(\mathbf{r}_1, \mathbf{r}_2, T/2) \rangle|^2, \tag{12}$$

where $\mathcal{A}$ is the antisymmetrization operator, the Coulomb wavefunctions ψ_E^l are calculated with $Z = 2$ and normalized on energy scale. The energy distribution is calculated by integrating the DI density of probability over $E_{k'}$ and summing over all (ℓ_1, ℓ_2) angular components [20]. We present the electron energy spectrum for TPDI of He for a photon energy of 2.2 au (60 eV) and various pulse durations. As expected, at a pulse duration of 34 au (822 as), sequential ionization dominates and the density of probability (full thin line) shows two peaks, close to the expected positions E_1 and E_2 (see figure 1), the peak widths being roughly given by the laser-bandwidth (about 0.37 au). The figure shows the dominant partial contributions associated with
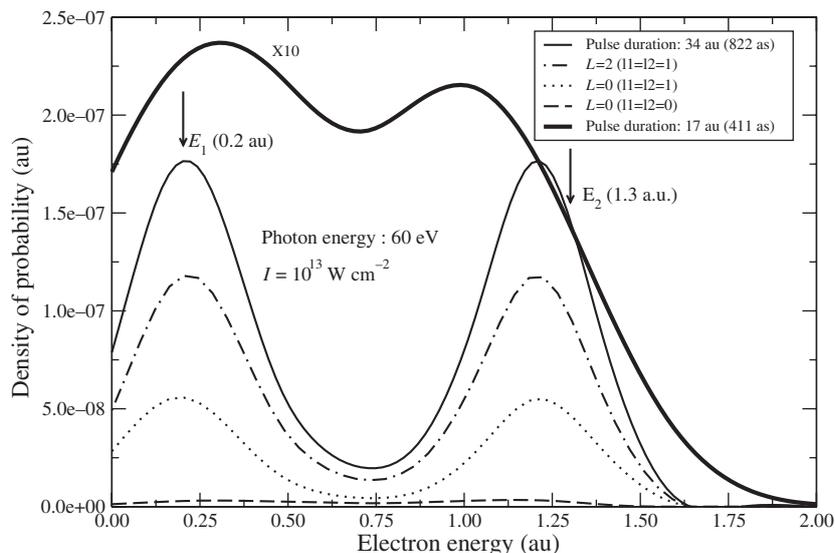
Figure 3. Electron energy spectrum for TPDI of helium in its ground state with $\hbar\omega = 2.2$ au. The total pulse duration is 34 au (822 as). The other laser parameters are indicated in the figure. The arrows indicate the expected position of the peaks in the sequential process (see figure 1). The figure shows the total density of probability and the density of probability calculated for selected angular components of the final state (we only show the three dominant contributions, see the insert). The thick curve represents the density of probability calculated for a total pulse duration of 17 au (411 as). It has been magnified by a factor of 10.

(ℓ_1, ℓ_2) pairs. As expected in the context of the sequential ionization, the contributions from the (1, 1) component dominates. The figure also shows (thick line) the density of probability for a pulse duration of $T = 17$ au (411 as). We note that the peaks are closer than in the previous case; they have moved towards each other. The pulse FWHM (205 as) is now of the order of the dielectronic interaction time defined above for helium (140 as). Therefore there is not enough time for the electron interaction energy E_{int} to be transferred to the first ejected electron before the escape of the second electron. As a consequence the peak E_2 is found at a lower energy, while the energy E_1 increases. Here, it is worth noting that the peak shift is much more pronounced than in the case of the sequential process (see figure 2). Therefore the shifts cannot be attributed to field bandwidth broadening. As a matter of fact, this effect should be observed for shorter wavelengths. This is illustrated in figure 4 which reports energy distributions for a photon energy of 3.2 au and pulse durations close to the previous case. For the longer pulse durations, the peaks are close to the expected positions E_1 and E_2 (see the figure). At $T \approx 16$ au the peaks shift towards each other, their separation in energy is about 0.6 au, in close agreement with the case reported in figure 3. Incidentally, we note that, although one-photon absorption takes the system above the DI threshold, the ${}^1P^o$ double continuum (populated through one-photon DI) plays a minor role in TPDI at this wavelength. This is fully coherent with our analysis above since the one-photon DI channel involves correlations beyond the zeroth order perturbation theory in $1/r_{12}$.
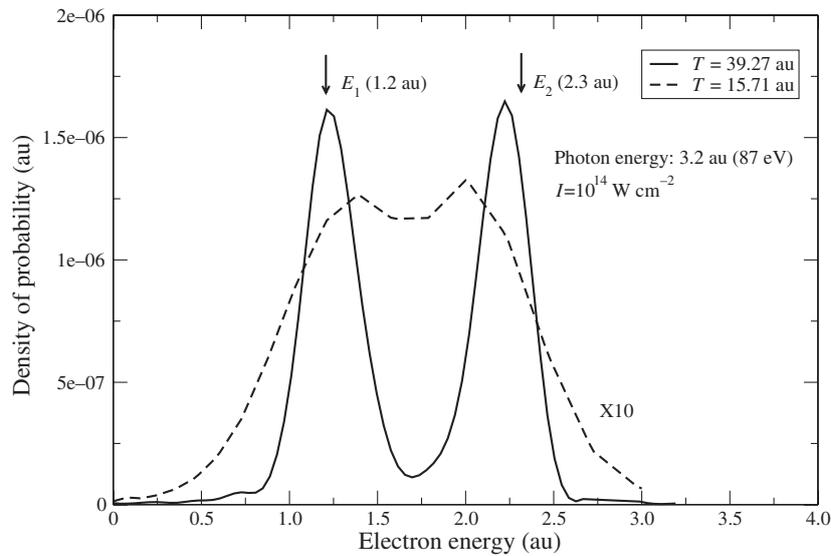
Figure 4. Electron energy spectrum for TPDI of helium in its ground state with $\hbar\omega = 3.2$ au. The total pulse durations are about 39 au (20 optical cycles) and 16 au (8 optical cycles). The other laser parameters are indicated in the figure. The distribution for $T \approx 16$ au has been magnified by a factor of 10.
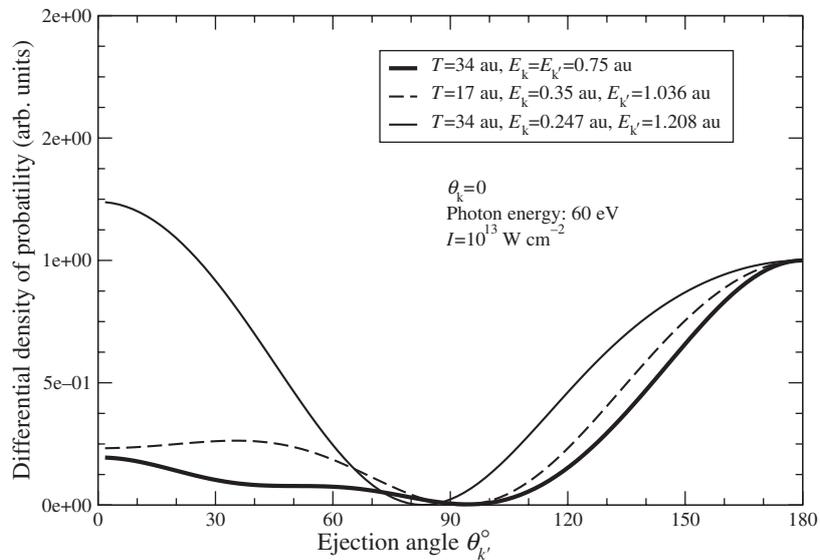

Figure 5. TPDI angular distributions calculated for various total pulse durations and electron energies (see the insert) with $\hbar\omega = 2.2$ au. One of the electrons is emitted along the z-axis ($\theta_k = 0$) with the energy E_k, the other electron is emitted with the energy $E_{k'}$. The curves are normalized to unity at $\theta_{k'} = 180°$.

Figure 5 shows the TPDI angular distribution calculated for various energies and pulse durations. This distribution $D_{\mathbf{k},\mathbf{k}'}$ has been calculated by projecting, at the end of the pulse, the total wavefunction on to a product of Coulomb functions (calculated with $Z = 2$ and fixed

wavevectors **k** and **k**′) representing the final state. The distribution reads:

$$D_{\mathbf{k},\mathbf{k}'} = |\langle \mathcal{A}(\psi_{\mathbf{k}}^-(\mathbf{r}_1)\psi_{\mathbf{k}'}^-(\mathbf{r}_2))|\Psi(\mathbf{r}_1, \mathbf{r}_2, T/2)\rangle|^2. \tag{13}$$

The final state is normalized on energy scale and it has 'ingoing' boundary conditions with $E_k = k^2/2$ and $E_{k'} = k'^2/2$. The wavefunctions $\psi_{\mathbf{k}}^-(\mathbf{r}_1)$ and $\psi_{\mathbf{k}'}^-(\mathbf{r}_2)$ are developed on to partial waves with angular momenta ℓ_1 and ℓ_2 [22]. The field having linear polarization and the polarization vector being aligned along the z-axis, the problem has cylindrical symmetry around z. For $T = 822$ as, this distribution has been calculated at the peak maxima ($E_k = 0.247$ au and $E_{k'} = 1.208$ au, see figure 3, thin line) and at $E_k = E_{k'} = 0.75$ au. In all cases one electron has a fixed energy E_k and is emitted in the direction $\theta_k = 0$, the other electron being emitted with the energy $E_{k'}$. At the peak maxima (thin full line) the angular distribution shows maxima at 0 and 180°, this agrees with a sequential emission of electrons with $\ell = 1$ angular momentum. By contrast with the direct process, most of the electrons are emitted at different times and the electron–electron interaction is dominated by the screening. The situation is different when $E_k = E_{k'} = 0.75$ au. The angular distribution has the character of direct DI (the electrons are emitted in opposite directions). In the latter case the electron repulsion plays a major role in the double electron ejection process since both electrons are emitted within a fraction of a femtosecond. Therefore, as predicted in earlier work [8], the DI in the energy region located in between the 'sequential' peaks has the signature of the direct process. Figure 5 also shows the angular distribution for the case $T = 411$ as at the position of the peaks maxima ($E_k = 0.35$ au and $E_{k'} = 1.036$ au, see figure 3, thick line). It is clear that the electrons are preferentially emitted in opposite directions, as in the case of direct DI. This is a further confirmation of our analysis: the shift of the peaks is not simply due to the peak broadening as the pulse duration shortens (although its effect is non-negligible), but it is related to the electron interaction dynamics. The experimental observation of the shift of the peaks remains, for the time being, extremely difficult at least in helium. However, as noted in the introduction, the measure of the momentum distribution of the recoil He^{2+} ion in COLTRIMS experiment is probably the best way to observe the effect. In the long pulse regime, the electrons being ejected with different energies and back-to-back or similar direction emission, the recoil ion momentum distribution should show maxima at positions different from zero. On the other hand, in the limit of ultra short pulse, the electrons tend to be emitted with roughly similar energies into opposite directions, the observed pattern should show a clear maximum at zero momentum.

4. Pump–probe processes

We now consider the interaction of helium with two XUV pulses. The results presented in this section for TPDI of He in its ground state have been obtained with the simple model described above and based on the lowest order time-dependent perturbation theory (see equation (7)). It is convenient to describe the total electric field as a sum of two pulsed fields shifted in time and characterized by different frequencies, phases and duration:

$$\vec{E} = [E_1 f_1(t) \sin(\omega_1 t + \phi_1) + E_2 f_2(t - D) \sin(\omega_2(t - D) + \phi_2)] \hat{z}, \tag{14}$$

where

$$f_j(t) = \cos^2\left(\frac{\pi}{T_j}t\right), \quad |t| \leqslant \frac{T_j}{2},$$

$$= 0, \quad |t| > \frac{T_j}{2}, \quad j = 1, 2. \tag{15}$$

Hereafter and for the sake of simplicity, we choose to label all the parameters associated with pulse p_j with the index j, $j = 1, 2$. T_1 and T_2 are the durations of p_1 and p_2 respectively while D is the time delay between the two pulses. D is defined as the distance between the maxima of p_2 and p_1. Therefore D is equal to 0 when the maxima of the two pulses coincide. ω_j, E_j, $f_j(t)$ and ϕ_j ($j = 1, 2$) denote, for each pulse, the photon frequency, the field amplitude, the envelope and the initial phase respectively. Let us denote the initial and final interaction times by $\mathcal{T}_i$ and $\mathcal{T}_f$, respectively. They are defined as follows:

$$\mathcal{T}_i = \min\left(-\frac{T_1}{2}, -\frac{T_2}{2} + D\right), \qquad \mathcal{T}_f = \max\left(\frac{T_1}{2}, \frac{T_2}{2} + D\right). \tag{16}$$

To probe the dynamics of the system, we 'play' with the delay time between p_1 and p_2. By changing the value of D, we can adjust the duration of the overlap between the two pulses whereas by changing the sign of D, we change the time order of these pulses. Figure 6 displays the electric field of the two pulses for different values of the time delay. In the present case, the expression of G in equation (8) becomes:

$$G(E_1, E_2, \omega_1, \omega_2, \phi_1, \phi_2, D, E_i, E_\alpha, E_f) =$$
$$\int_{\mathcal{T}_i}^{\mathcal{T}_f} dt\{E_1 f_1(t) \sin(\omega_1 t + \phi_1) + E_2 f_2(t - D) \sin(\omega_2(t - D) + \phi_2)\}e^{i(\omega_{f\alpha})t}$$
$$\times \int_{\mathcal{T}_i}^{t} d\tau\{E_1 f_1(\tau) \sin(\omega_1 \tau + \phi_1) + E_2 f_2(\tau - D) \sin(\omega_2(\tau - D) + \phi_2)\}e^{i(\omega_{\alpha i})\tau}.$$
$$\tag{17}$$

In all the results presented in this section the frequencies of the two XUV pulses are fixed: $\omega_1 = 1.3$ au and $\omega_2 = 2.1$ au. In figure 7, we show the electron energy distribution for TPDI of helium in its ground state by the two XUV pulses for different values of the time delay D between the pulses. The total duration of each pulse is $T_1 = 12$ optical cycles (1.4 fs) and $T_2 = 14$ optical cycles (1 fs). The peak intensities of the pulses p_1 and p_2 are equal to 10^{14} and 10^{13} W cm^{-2}. For long and positive values of the time delay D, there is no overlap between the two pulses p_1 and p_2. The system interacts first with p_1 leading to a single ionization peak at $E_1 = 0.4$ au. The second pulse p_2 with a frequency 2.1 au can ionize the residual ion which was left in its ground state after the first photon absorption. Consequently, the TPDI process is necessarily sequential and the first outgoing electron carries all the dielectronic interaction energy as in a single pulse event [8]. When the time delay becomes shorter, the two pulses begin to overlap. In that case, a new process becomes possible, namely the successive absorption of photons of 2.1 and 1.3 au. However, this new two-color process is only possible if the residual ion has no time to relax before the absorption of the photon of 1.3 au. In other words, this process must be direct in order to occur. In this case both electrons share the dielectronic interaction energy. This leads to the shift of the two peaks observed in figure 7 for $D = 1.61$ au and $D = -3.22$ au. For long and negative values of the time delay and a non zero overlap
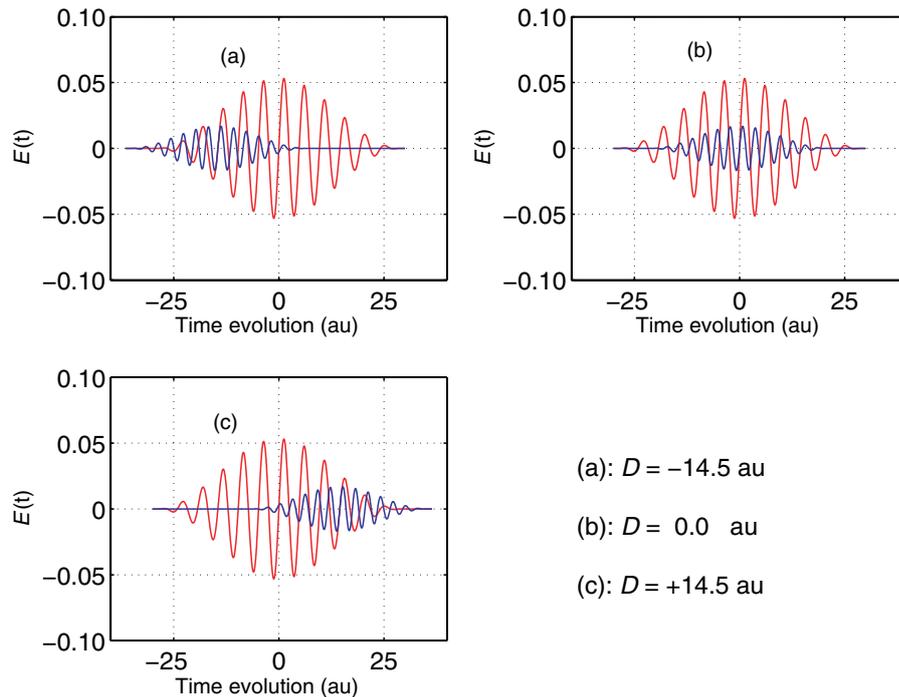
Figure 6. Electric field associated with the pulses p_1 and p_2. Three values ((a)–(c)) of the time delay D between the two pulses are considered. The pulse characteristics are: $I_1 = 10^{14}$ W cm^{-2}, $\omega_1 = 1.3$ au, $T_1 = 12$ cycles, $I_2 = 10^{13}$ W cm^{-2}, $\omega_2 = 2.1$ au, and $T_2 = 14$ cycles. The red curve corresponds to $E_1(t)$ and the blue one to $E_2(t)$.

between the two pulses, this new direct two-color process becomes progressively the dominant one leading to a single peak around $E_1 = E_2 = 7$ eV in the electron energy distribution (see the full green curve in figure 7). For long and negative time delays, without overlap between the pulses, the system interacts first with the pulse p_2. Because the interaction of p_1 with He cannot lead to TPDI, the electron energy distribution exhibits two very small peaks at $E_1 = 2.7$ eV and $E_2 = 33$ eV.

In figure 8, we show the TPDI probability as a function of the duration of the pulse p_2 in a situation where the time delay D is fixed and equal to -150 au. We also fix the pulse duration of p_1 to 24 optical cycles (2.8 fs) while the duration of p_2 varies from 10 au (242 as) up to 70 au (1.7 fs). Therefore the pulse p_2 always interacts with He before the pulse p_1 and there is no overlap between the two pulses. The peak intensities of pulses p_1 and p_2 are equal to 5×10^{13} and 10^{13} W cm^{-2}, respectively. The blue curve in figure 8 has been obtained when the pulse p_1 is switched off. In this case, and for long pulse durations T_2, the DI process is mainly sequential and the DI probability varies like T_2^2. The red curve has been obtained with the two pulses. The first pulse p_2 ionizes the system while the second one (p_1 in this case) 'probes' the initial photoionization process. For short values of T_2 (the duration of p_2), the residual ion is left in a linear superposition of He$^+$ eigenstates (i.e. in an unrelaxed ion state) after the first electron ejection. The second pulse p_1 with frequency ω_1 can then ionize the 'unrelaxed' residual ion. This explains why the TPDI probability is much larger in the presence of the pulse p_1 even if they do not overlap. Note that a linear superposition of states can only relax in the presence of
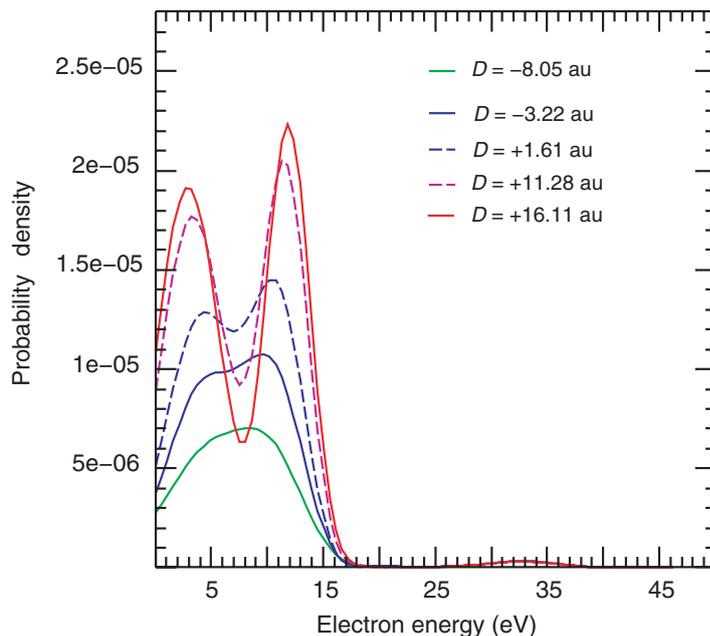
Figure 7. Electron energy distribution for TPDI of helium in its ground state by a two-color electromagnetic field. The pulse parameters are: $I_1 = 10^{14}$ W cm^{-2}, $\omega_1 = 1.3$ au, $T_1 = 12$ cycles, $I_2 = 10^{13}$ W cm^{-2}, $\omega_2 = 2.1$ au, and $T_2 = 14$ cycles. Various time delays D between the two pulses are considered; they are indicated in the figure.

an external field. When the duration of p_2 becomes larger, the residual ion has time to relax into its ground state. As a result, the pulse p_1 cannot ionize the He$^+$ from its ground state and the only process which can occur is the TPDI process with the pulse p_2. This is why the two curves coincide for large values of T_2.

In figure 9, we present the TPDI probability as a function of the time delay between the pulses. The peak intensities are the same as in the previous case (figure 8). The pulse duration T_2 is fixed and equal to 16 optical cycles (≈ 1.2 fs) and the duration of p_1 takes two different values: 24 optical cycles, i.e. 2.8 fs (red curve) and 48 optical cycles (blue curve). For large negative values of the time delay, it is only the pulse p_2 that contributes since its duration is large enough to allow the complete relaxation of the residual ion into its ground state. Once both pulses overlap completely, it is the sequential absorption of a photon of 1.3 au and a photon of 2.1 au which is by far the dominant process. In the latter context the DI probability depends on the number of He$^+$ ions due to the absorption by He of the first photon of 1.3 au *before* the interaction with p_2. In fact this number of He$^+$ ions is directly proportional to the intensity profile of p_1 integrated from $\mathcal{T}_i = -T_1/2$ up to D. This explains the quasi linear behavior of the DI probability around $D = 0$. As a matter of fact, the dependence on D will be exactly linear in the case of square pulses. For long positive time delays D, when both pulses no longer overlap, the TPDI probability becomes a constant as expected; in this case, the integration of the intensity profile of pulse p_1 is performed over its total duration. Note that if the duration of pulse p_1 is multiplied by a factor 2 (see the blue curve) the TPDI probability is also multiplied by a factor 2.
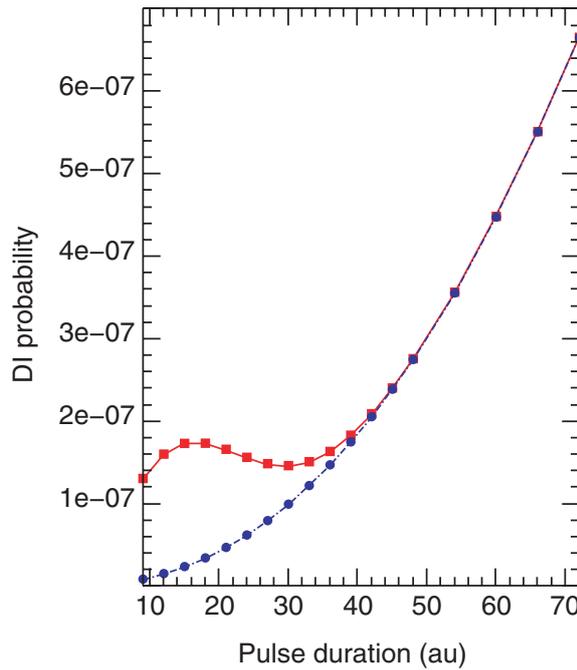
Figure 8. TPDI probability as a function of the pulse duration T_2. The red curve is obtained when the two pulses are present. The pulse parameters are: $I_1 = 5 \times 10^{13}$ W cm^{-2}, $\omega_1 = 1.3$ au, $T_1 = 24$ cycles, $I_2 = 10^{13}$ W cm^{-2}, $\omega_2 = 2.1$ au. The time delay between the two pulses is -150 au. The blue curve represents the DI probability when only the pulse p_2 is present.

On the basis of the above discussion we could write the TPDI probability as follows:

$$P_{\mathrm{di}} = \alpha T_2^2 + \beta T_1 T_2, \tag{18}$$

where α and β are quantities that depend on the time delay D. In this expression, the first term αT_2^2 is the main contribution when the time delay is lower than $-T_2/2 - T_1/2$. But when $|D| \approx 0$ or $D > 0$, it becomes negligible compared to the second term $\beta T_1 T_2$ which is associated with the sequential two-color process. However, because this latter process is in fact the combination of two single ionization events, it is easy to show that the TPDI probability is actually proportional to the energy carried by each pulse rather than to the pulse durations T_1 and T_2. As a result, the measure of this probability does not provide direct information on the duration of the shortest pulse (p_2 in the present case).

5. Conclusion

In this contribution, we have considered the TPDI of He in its ground state and have focused our analysis on the electron dynamics on the attosecond timescale. We first treated the case of the interaction of He with a single pulse and studied how the electron correlations affect the electron energy and angular distributions. In the direct regime, the angular correlations favor a back-to-back emission along the polarization axis whereas dynamical screening, i.e. the radial correlations, leads to an equal energy sharing. In the sequential regime, the electron energy distribution exhibits two peaks separated by the dielectronic interaction energy. When
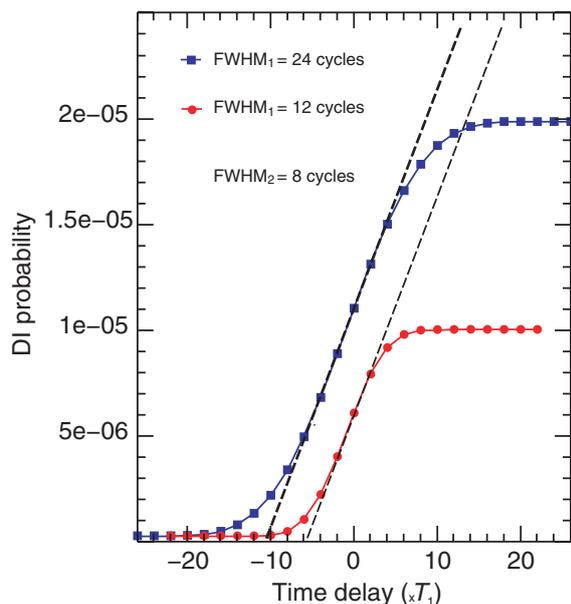
Figure 9. TPDI probability as a function of the time delay in units of T_1 between the pulses. The pulse parameters are: $I_1 = 5 \times 10^{13}$ W cm^{-2}, $\omega_1 = 1.3$ au, $I_2 = 10^{13}$ W cm^{-2}, $\omega_2 = 2.1$ au, and $T_2 = 16$ cycles. Two values of the pulse duration of p_1 are considered: 24 and 48 cycles. The parallel dotted lines emphasize the linear dependence of the DI probability on the time delay around zero when the two pulses completely overlap.

the energy sharing corresponds to one of the peaks, both electrons are either emitted in the same direction or back-to-back along the polarization axis. At equal energy sharing, the back-to-back emission dominates. In the transient regime, when the pulse duration becomes of the order of the dielectronic interaction time, the two peaks observed in the sequential regime move towards each other and the back-to-back emission becomes the dominant process as in the direct regime. In the second part of this contribution, we have considered the interaction of He with two XUV pulses of different frequency, intensity and duration. By using relatively long pulses and by playing with the time delay between the pulses, we show that a similar dynamical effect in the electron energy distribution, i.e. the shift of the peaks towards each other until they merge completely, can be observed. Furthermore, in the case where one of the pulses is long with a photon energy much lower than 2 au and the other one is ultrashort with a frequency higher than 2 au, the DI probability as a function of the ultrashort pulse duration exhibits a clear signature of the relaxation time of He$^+$. This is true provided that helium interacts with the ultrashort pulse first. This provides an upper bound of the relaxation time of He$^+$ and indirectly some information on the duration of the shortest pulse. Finally, we studied the TPDI as a function of the time delay between the two pulses which have the same frequency as before but a much longer duration. Note that, in the context of extreme ultraviolet, techniques based on the outcome of the two-photon processes in He have already been used to extract information on the duration of sub-femtosecond pulses [23, 24]. However, in the present case, the fact that the dominant (two-color) process is sequential prevents such information being extracted, since in a real experiment it is the energy of the pulse rather than its actual peak intensity which is measured.

IOP Institute of Physics   **Φ** DEUTSCHE PHYSIKALISCHE GESELLSCHAFT

Acknowledgments

References

[1] Agostini P and Dimauro L 2004 *Rep. Prog. Phys.* **67** 813
[2] Kienberger R *et al* 2004 *Nature* **427** 817
    Goulielmakis E *et al* 2004 *Science* **305** 1267
    Sansone G *et al* 2006 *Science* **314** 443
    Schultze M *et al* 2007 *New J. Phys.* **9** 243
[3] Drescher M, Hentschel M, Klenberger R, Ulberacker M, Yakoviev V, Scrinzi A, Westerwalbesloh Th, Kleineberg U, Heinzmann U and Krausz F 2002 *Nature* **419** 803
[4] Horner D A, Morales F, Rescigno T N, Martín F and McCurdy C W 2007 *Phys. Rev.* A **76** 030701
[5] Hasegawa H, Takahashi E J, Nabekawa Y, Ishikawa K L and Midorikawa K 2005 *Phys. Rev.* A **71** 023407
[6] Sorokin A A, Wellhöfer M, Bobashev S V, Tiedtke K and Richter M 2007 *Phys. Rev.* A **75** 051402
[7] Moshammer R *et al* 2007 *Phys. Rev. Lett.* **98** 203001
[8] Bachau H and Lambropoulos P 1991 *Phys. Rev.* A **44** R9
[9] Foumouo E, Laulan S, Piraux B and Bachau H 2006 *J. Phys. B: At. Mol. Opt. Phys.* **39** 427
[10] Madsen L B 2002 *Phys. Rev.* A **65** 053417
[11] Foumouo E, Lagmago Kamta G, Edah G and Piraux B 2006 *Phys. Rev.* A **74** 063409
[12] Lagmago Kamta G, Piraux B and Scrinzi A 2001 *Phys. Rev.* A **63** 040502
[13] Bachau H, Cormier E, Decleva P, Hansen J E and Martín F 2001 *Rep. Prog. Phys.* **64** 1815
[14] Heller E J and Yamani H A 1974 *Phys. Rev.* A **9** 1201
[15] Foumouo E, Antoine Ph, Piraux B, Malegat L, Bachau H and Shakeshaft R *J. Phys. B: At. Mol. Opt. Phys.* submitted
[16] Rau A R P 1971 *Phys. Rev.* A **4** 207
[17] Nikolopoulos L A A and Lambropoulos P 2007 *J. Phys. B: At. Mol. Opt. Phys.* **40** 1347
[18] Piraux B, Bauer J, Laulan S and Bachau H 2003 *Eur. Phys. J.* D **26** 7
[19] Laulan S, Bachau H, Piraux B, Bauer J and Lagmago Kamta G 2003 *J. Mod. Opt.* **50** 353
[20] Laulan S and Bachau H 2003 *Phys. Rev.* A **68** 013409
[21] Laulan S and Bachau H 2004 *Phys. Rev.* A **69** 033408
[22] Landau L D and Lifshitz E 1965 *Quantum Mechanics* 2nd edn (New York: Pergamon)
[23] Sekikawa T, Kosuge A, Kanai T and Watanabe S 2004 *Nature* **432** 605
[24] Kosuge A, Sekikawa T, Zhou X, Kanai T, Adachi S and Watanabe S 2006 *Phys. Rev. Lett.* **97** 263901